

Available online at [www.sciencedirect.com](http://www.sciencedirect.com)

SciVerse ScienceDirect

[www.elsevier.com/locate/matchar](http://www.elsevier.com/locate/matchar)

# Dislocation evolution in 316 L stainless steel during multiaxial ratchetting deformation

Yawei Dong<sup>a</sup>, Guozheng Kang<sup>a,\*</sup>, Yujie Liu<sup>b</sup>, Hong Wang<sup>b</sup>, Xiaojuan Cheng<sup>b</sup>

<sup>a</sup>State Key Laboratory of Traction Power, Southwest Jiaotong University, Chengdu 610031, China

<sup>b</sup>School of Mechanics and Engineering, Southwest Jiaotong University, Chengdu 610031, China

## ARTICLE DATA

### Article history:

Received 16 July 2011

Received in revised form

22 December 2011

Accepted 4 January 2012

### Keywords:

316 L stainless steel

Ratchetting

Dislocation pattern

Multiaxial cyclic loading

Microscopic observation

## ABSTRACT

Dislocation patterns and their evolutions in 316 L stainless steel during the multiaxial ratchetting deformation were observed by transmission electron microscopy (TEM). The microscopic observations indicate that the dislocation evolution presented during the multiaxial ratchetting with four kinds of multiaxial loading paths is similar to that in the uniaxial case [G. Z. Kang et al., Mater Sci Eng A 527 (2010) 5952]. That is, dislocation networks and dislocation tangles are formed quickly by the multiple-slip and cross-slip of dislocation activated by applied multiaxial stress; and then polarized patterns such as dislocation walls and elongated incipient dislocation cells are formed at the last stage of multiaxial ratchetting. The dislocation patterns evolve more quickly from the modes at low dislocation density to the ones at high density during the multiaxial ratchetting than that in the uniaxial case, and some traces of multiple-slip are observed in the multiaxial ones. The dislocation evolution during the multiaxial ratchetting deformation is summarized by comparing the observed dislocation patterns with those presented in the multiaxial strain-controlled and symmetrical stress-controlled cyclic tests. The multiaxial ratchetting of 316 L stainless steel can be microscopically and qualitatively explained by the observed evolution of dislocation patterns.

© 2012 Elsevier Inc. All rights reserved.

## 1. Introduction

In the previous work of the authors [1], dislocation patterns and their evolutions in 316 L stainless steel during the uniaxial ratchetting deformation were observed by transmission electron microscopy (TEM) and the micro-mechanism of uniaxial ratchetting was discussed qualitatively by referring to the work done by Bocher et al. [2] and Gaudin and Feaugas [3]. However, only the uniaxial case was addressed there [1], and the dislocation patterns and their evolutions during the multiaxial ratchetting deformation with various loading paths have not been discussed yet. It is well-known that the multiaxial ratchetting differs from the uniaxial one, especially for the non-proportional multiaxial ratchetting, as reviewed in [4,5]. It is necessary to

discuss the microscopic physical nature of multiaxial ratchetting by observing the dislocation patterns and their evolutions.

The physical mechanism of plastic deformation in many engineering materials has been studied by many authors [6–17] through observing the dislocation patterns and their evolution during the plastic deformation. Most of previous researches were performed to reveal the micro-mechanism of uniaxial and multiaxial low-cycled fatigue, no ratchetting was addressed. The dislocation patterns during the multiaxial ratchetting deformation were first observed by Bocher et al. [2] for 316 L stainless steel and with some combined stress–strain controlled multiaxial loading paths. However, they mainly addressed the dislocation patterns at the end of cyclic loading and within 300 cycles. The dislocation evolution at different

\* Correspondent author: Tel.: +86 28 87603794; fax: +86 28 87600797.  
E-mail address: [guozhengkang@yahoo.com.cn](mailto:guozhengkang@yahoo.com.cn) (G. Kang).

stages of multiaxial ratchetting deformation and with higher number of cycles has not been discussed in detail yet in [2].

Therefore, similar to the previous work [1], the dislocation patterns and their evolution during the multiaxial ratchetting deformation were observed by TEM for 316 L stainless steel and with four kinds of loading paths in this work. The dislocation evolution during the multiaxial ratchetting deformation was discussed by comparing the dislocation patterns observed at different stages of ratchetting deformation with those obtained in the symmetrical multiaxial strain-controlled cyclic loading cases. Some conclusions significant to investigate the micro-mechanism of multiaxial ratchetting are obtained.

## 2. Experimental Procedure

The experimental material is polycrystalline 316 L austenitic stainless steel experienced a solution treatment (i.e., kept at 1050 °C for 60 min, and then cooled in water), and is the same as that used in the previous work [1]. The chemical composition of 316 L stainless steel is (in mass percentage): C, 0.016; Mn, 1.422; Si, 0.71; P, 0.05; Ni, 11.25; Cr, 18.05; Mo, 2.583; Ne, 0.013; Fe, remained.

Tubular specimens with an outside diameter of 16 mm and inner diameter of 13 mm were used in multiaxial cyclic tests. The multiaxial strain-controlled and stress-controlled cyclic tests were carried out on MTS809-250KN; and the loading process was controlled and the experimental data were collected by Teststar control system. The axial and torsional strains were measured by a tension-torsion extensometer, whose limited axial strain was 10% and torsional angle ranged from  $-5^\circ$  to  $+5^\circ$ . No thermal treatment was performed after the specimen had been machined. In order to consider the effect of multiaxial loading path on the multiaxial ratchetting of 316 L stainless steel, four kinds of loading paths were adopted in the tests. The multiaxial loading paths prescribed in the multiaxial strain and stress-controlled cycling tests are given in Figs. 1 and 2, respectively. In this work, the applied strain rate in strain-controlled cyclic test is set as  $4 \times 10^{-3}/s$ , and the applied stress rate in stress-controlled cyclic one is 300 MPa/s. The applied multiaxial strain amplitudes are prescribed as following: (1) Pure shear path (Fig. 1a): equivalent shear strain amplitude of  $\pm 0.6\%$ ; (2)  $45^\circ$  linear path (Fig. 1b):  $\pm 0.4243\%$  in both the axial and torsional directions; (3) Rhombic and circular paths (Fig. 1c and d):  $\pm 0.4\%$  in both the axial and torsional directions. The loading conditions for multiaxial ratchetting tests are set as: (1) circular (Fig. 2a) and its

inscribed rhombic (Fig. 2c) paths, equivalent shear stress amplitude of  $\pm 350$  MPa in the torsional direction, but  $70 \pm 350$  MPa (i.e., the axial mean stress is 70 MPa and stress amplitude is 350 MPa) in the axial direction, respectively; (2) inscribed  $30^\circ$  linear path (Fig. 2b), equivalent shear stress amplitude of  $\pm 175$  MPa in the torsional direction, but  $70 \pm 303.11$  MPa in the axial direction; (3) inscribed butterfly-typed (Fig. 2d) paths, equivalent shear stress amplitude of  $\pm 247.5$  MPa in the torsional direction, but  $70 \pm 247.5$  MPa in the axial direction (for the symmetrical case,  $\pm 247.5$  MPa).

Similar to the previous work [1], thin foils for transmission electron microscopy (TEM) observation were made from the mechanically polished films by electro-polishing in a twin jet apparatus. The films were obtained from the lamellae cut directly from the tested tubular specimens in the direction parallel to the axes. The electrolyte used in the electro-polishing consisted of 10%  $HNO_3$  and 90%  $CH_3CH_2OH$ , and the controlling parameters were: a voltage of 30 to 50 V, current of 80 to 100 mA and temperature of  $-10$  to  $-20$  °C. The microscopic observations were performed by F20 Field Emission Transmission Electron Microscopy (FE-TEM), and the operating voltage was 200 kV.

## 3. Experimental Results and Discussion

Firstly, the dislocation patterns and their evolutions during the uniaxial ratchetting of 316 L stainless steel observed in the previous work [1] are outlined as follows in order to compare them with those presented during the multiaxial ratchetting:

- (1) During the uniaxial ratchetting deformation (i.e., applied stress amplitude is 350 MPa and mean stress is 70 MPa), dislocation density increases progressively and dislocation configuration gradually evolves from low-density patterns such as dislocation lines, pile-ups, and light dislocation tangles to higher-density ones such as heavy dislocation tangles, walls and veins, and finally dislocation cells. No twins and strain-induced martensite phases are observed within the prescribed number of cycles.
- (2) At the stage I of uniaxial ratchetting, dislocation density increases greatly with the increasing number of cycles and the hardening caused by the increased dislocation density makes the ratchetting strain rate decreased continuously. At the stage II, dislocation patterns

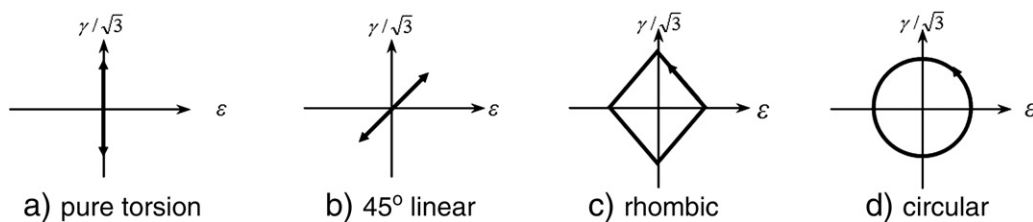


**Fig. 1 – Loading paths used in the multiaxial strain-controlled cyclic tests with loading conditions as follows: (a) equivalent shear strain amplitude of  $\pm 0.6\%$  in torsional direction; (b) equivalent strain amplitude of  $\pm 0.4243\%$  in both axial and torsional directions; (c) and (d) equivalent strain amplitude of  $\pm 0.4\%$  in both axial and torsional directions.**

Download English Version:

<https://daneshyari.com/en/article/1571470>

Download Persian Version:

<https://daneshyari.com/article/1571470>

[Daneshyari.com](https://daneshyari.com)